

## Synthesis, Characterization, and Crystal Structures of Two Divalent Metal Diphosphonates with a Layered and a 3D Network Structure

Jiang-Gao Mao, Zhike Wang, and Abraham Clearfield\*

Department of Chemistry, Texas A&M University, P.O. Box 30012,  
College Station, Texas 77843-3255

Received November 26, 2001

Reactions of *N*-methyliminobis(methylenephosphonic acid),  $\text{CH}_3\text{N}(\text{CH}_2\text{PO}_3\text{H}_2)_2$  ( $\text{H}_4\text{L}$ ), with divalent metal acetates under different conditions result in metal diphosphonates with different structures.  $\text{Mn}(\text{H}_3\text{L})_2 \cdot 2\text{H}_2\text{O}$  (complex **1**) with a layer structure was prepared by a layering technique. It is triclinic,  $P\bar{1}$ , with  $a = 9.224(3)$  Å,  $b = 9.780(3)$  Å,  $c = 10.554(3)$  Å,  $\alpha = 82.009(6)^\circ$ ,  $\beta = 74.356(6)^\circ$ ,  $\gamma = 89.853(6)^\circ$ ,  $Z = 2$ . The Mn(II) ion is octahedrally coordinated by six phosphonate oxygen atoms from four ligands, two of them in a bidentate and two in a unidentate fashion. Each  $\text{MnO}_6$  octahedron is further linked to four neighboring  $\text{MnO}_6$  octahedra through four bridging phosphonate groups, resulting in a two-dimensional metal phosphonate (002) layer. These layers are held together by strong hydrogen bonds between uncoordinated phosphonate oxygen atoms. The zinc complex  $\text{Zn}_3(\text{HL})_2$  (complex **2**) was synthesized by hydrothermal reactions (4 days, 438 K, autogenous pressure). It is monoclinic,  $P2_1/n$  with  $a = 7.7788(9)$  Å,  $b = 17.025(2)$  Å,  $c = 13.041(2)$  Å,  $\beta = 94.597(2)^\circ$ ,  $Z = 4$ . The structure of complex **2** features a 3D network built from  $\text{ZnO}_4$  tetrahedra linked together by bridging phosphonate groups. Each zinc cation is tetrahedrally coordinated by four phosphonate oxygen atoms from four ligands, each of which connects with six zinc atoms, resulting in voids of various sizes. Magnetic measurements for the manganese complex shows an antiferromagnetic interaction at low temperature. The effect of the extent of deprotonation of phosphonic acids on the type of complex formed is discussed.

### Introduction

Metal phosphonate chemistry has attracted attention in recent years due to potential applications in the areas of catalysis, ion exchange, proton conductivity, intercalation chemistry, photochemistry, and materials chemistry.<sup>1</sup> Most of the compounds studied are layered species in which the metal octahedra are bridged by phosphonic acid tetrahedra to form two-dimensional layers that are separated by the hydrophobic regions of the organic moieties.<sup>1</sup> Studies from our group and from others have shown that a variety of metal ions, including group 4 and 14 elements and divalent and trivalent ions, form this type of layered compound.<sup>1–3</sup>

Research on metal complexes with phosphonic acids attached with aza-crown ethers show that those compounds have many unusual structural features.<sup>1,4</sup> Phosphonic acids with functional carboxylate groups, such as *N*-(phosphonomethyl)-iminodiacetic acid ( $\text{H}_4\text{PMIDA}$ ) are also interesting, since they can adopt various kinds of coordination modes under different reaction conditions. A mixed phosphate–phosphonate layered zirconium compound was made by reaction of a zirconium salt with a mixture of phosphoric acid and  $\text{H}_4\text{PMIDA}$  solutions.<sup>5</sup> When the above reactions were carried

\* Author to whom correspondence should be addressed. E-mail: clearfield@mail.chem.tamu.edu.

(1) (a) Stein, E.; Clearfield, A.; Subramanian, M. A. *Solid State Ionics* **1996**, *83*, 113. (b) Alberti, G.; Costantino, U. In *Comprehensive Supramolecular Chemistry*; Lehn, J. M., Ed.; Pergamon-Elsevier Science Ltd.: London, 1996; p 1. (c) Clearfield, A. *Curr. Opin. Solid State Mater. Sci.* **1996**, *1*, 268. (d) Clearfield, A. Metal phosphonate chemistry. In *Progress in Inorganic Chemistry*; Karlin, K. D., Ed.; John Wiley & Sons: New York, 1998; Vol. 47, pp 371–510 and references therein.

(2) Thompson, M. E. *Chem. Mater.* **1994**, *6*, 1168.  
(3) Alberti, G.; Costantino, U. In *Comprehensive Supramolecular Chemistry*; Lehn, J. M., Ed.; Pergamon-Elsevier Science Ltd.: London, 1996; p 151.  
(4) (a) Zhang, B.; Clearfield, A. *J. Am. Chem. Soc.* **1997**, *119*, 2751. (b) Sharma, C. V. K.; Clearfield, A. *J. Am. Chem. Soc.* **2000**, *122*, 1558. (c) Lukes, I.; Kotek, J.; Vojtisek, P.; Hermann, P. *Coord. Chem. Rev.* **2001**, *216–217*, 287. (d) Clearfield, A.; Poojary, D. M.; Zhang, B.; Zhao, B.; Derecskei-Kovacs, A. *Chem. Mater.* **2000**, *12*, 2745.  
(5) (a) Zhang, B.; Poojary, D. M.; Clearfield, A.; Peng, G.-Z. *Chem. Mater.* **1996**, *8*, 1333. (b) Poojary, D. M.; Clearfield, A. *J. Organomet. Chem.* **1996**, *512*, 237. (c) Poojary, D. M.; Zhang, B.; Clearfield, A. *Angew. Chem., Int. Ed. Engl.* **1994**, *33*, 2324.

out in the absence of phosphoric acid, a linear chain compound was isolated.<sup>6</sup> In both cases the iminodiacetic moieties are only involved in hydrogen bonding. Under less acidic conditions, we isolated two novel complexes,  $[\text{Co}_2(\text{PMIDA})(\text{H}_2\text{O})_5]\cdot\text{H}_2\text{O}$ , whose structure contains double layers of Co(II) carboxylate interconnected by layers of Co(II) phosphonate, and a zinc carboxylate–phosphonate hybrid layered complex,  $\text{Zn}_2(\text{PMIDA})(\text{CH}_3\text{CO}_2\text{H})\cdot 2\text{H}_2\text{O}$ .<sup>7</sup> With the complete deprotonation by adding potassium hydroxide, Wood and co-workers obtained the canted anti-ferromagnet  $\{\text{K}_2\text{Co}(\text{PMIDA})\}_6\cdot x\text{H}_2\text{O}$ , whose crystal structure features a hexameric ring in the chair conformation.<sup>8</sup> Diphosphonic acids in which the two phosphonate groups are connected by alkyl or aromatic organic matrixes are important since they can form pillared layered phosphonates with divalent transition metal,<sup>9</sup> titanium(IV),<sup>10</sup> and zirconium(IV).<sup>11</sup> Diphosphonic acids in which the two phosphonate groups are attached to diamine groups ( $\text{HO}_3\text{PCH}_2\text{HNRNHCH}_2\text{PO}_3\text{H}$ ) can form metal phosphonates with a variety of structures, such as mononuclear chelate complexes,<sup>12</sup> complexes with 1D chain structure or 3D network structure based on dimeric units,<sup>13</sup> and pillared layered compounds.<sup>4,14</sup> Only a few structural studies have been done on metal complexes of aminodiphosphonic acids,  $\text{RN}(\text{CH}_2\text{PO}_3\text{H}_2)_2$ .<sup>15,16</sup> The crystal structure of a copper complex with ethylaminebis-(methylphosphonate) was reported by Makaranets et al.<sup>15</sup> Recently the *N*-methyliminodi(methylenephosphonate) was structurally determined, and its coordination behavior with metal ions has been studied in aqueous solution by potentiometric titration and NMR measurements. Its zinc complex was proposed to be a layered structure.<sup>16</sup> We deem that much more work is needed in order to understand the structures of these metal phosphonates in the solid state. Herein we report the synthesis, characterization, and crystal structures of two new divalent metal complexes with *N*-methyliminobis(methylenephosphonic acid), namely,  $\text{Mn}(\text{H}_3\text{L})_2\cdot 2\text{H}_2\text{O}$  (complex **1**), with a layer structure, and  $\text{Zn}_3(\text{HL})_2$  (complex **2**), whose structure features a 3D network; both structure types were not predicted by the solution studies.

- (6) Zhang, B.; Poojary, D. M.; Clearfield, A. *Inorg. Chem.* **1998**, *37*, 249.  
 (7) Mao, J.-G.; Clearfield, A. *Inorg. Chem.*, submitted.  
 (8) Gutschke, S. O. H.; Price, D. J.; Powell, A. K.; Wood, P. T. *Angew. Chem., Int. Ed.* **1999**, *38*, 1088.  
 (9) (a) Poojary, D. M.; Zhang, B.; Clearfield, A. *J. Am. Chem. Soc.* **1997**, *119*, 12550. (b) Zhang, B.; Poojary, D. M.; Clearfield, A. *Inorg. Chem.* **1998**, *37*, 1844. (c) Poojary, D. M.; Zhang, B.; Clearfield, A. *Chem. Mater.* **1999**, *11*, 421.  
 (10) Serre, C.; Férey, G. *Inorg. Chem.* **2001**, *40*, 5350.  
 (11) (a) Alberti, G.; Vivani, R.; Mascarós, M. S. *J. Mol. Struct.* **1998**, *470*, 81. (b) Alberti, G.; Costantino, U.; Marmottini, F.; Vivani, R.; Zappelli, P. *Microporous Mesoporous Mater.* **1998**, *21*, 297.  
 (12) Shkol'nikova, L. M.; Poznyak, A. L.; Bel'skii, V. K.; Rudomino, M. V.; Dyatlova, N. M. *Koord. Khim.* **1986**, *12*, 981.  
 (13) (a) Song, H.-H.; Zheng, L.-M.; Wang, Z.-M.; Yan, C.-H.; Xin, X.-Q. *Inorg. Chem.* **2001**, *40*, 5024. (b) Choi, N.; Khan, I.; Matthews, R. W.; McPartlin, M.; Murphy, B. P. *Polyhedron* **1994**, *13*, 847. (c) LaDuca, R.; Rose, D.; DeBord, J. R. D.; Haushalter, R. C.; O'Connor, C. J.; Zubieta, J. *J. Solid State Chem.* **1996**, *123*, 408.  
 (14) Soghomonian, V.; Diaz, R.; Haushalter, R. C.; O'Connor, C. J.; Zubieta, J. *Inorg. Chem.* **1995**, *34*, 4460.  
 (15) Makaranets, B. I.; Polynova, T. N.; Mitrofanova, N. D.; Porai-Koshits, M. A. *J. Struct. Chem.* **1991**, *32*, 94.  
 (16) Matczak-Jon, E.; Kurzak, B.; Kamecka, A.; Sawka-Dobrowolska, W.; Kafarski, P. *J. Chem. Soc., Dalton Trans.* **1999**, 3627.

## Experimental Section

**Materials and Methods.** Deionized water used in all experiments was purified to a resistivity of 17.6 MΩ cm with a Barnstead Nanopure II system. All other chemicals were of reagent grade quality obtained from commercial sources and used without further purification. Solution NMR was recorded on a Varian Unity Plus 300 spectrometer.  $\text{H}_3\text{PO}_4$  (EM Science, 85%) was used as  $^{31}\text{P}$  standard reference. The  $^{31}\text{P}$  solid MAS NMR spectrum was obtained on a Bruker MSL-300 unit. Elemental analysis data were obtained from Desert Analytics, Tucson, AZ. Thermogravimetric analysis was carried out with a TA 4000 unit, at a heating rate of 10 °C/min under an oxygen atmosphere. X-ray powder data for the samples were collected with a Rigaku computer-automated diffractometer. The X-ray source was a rotating anode operating at 50 kV and 100 mA with a copper target and graphite-monochromated radiation. The magnetic measurements were performed on polycrystalline samples of complex **1** sealed in a plastic bag in an inert atmosphere with a SQUID susceptometer (Quantum Design, MPMS-XL-5) in the temperature range of 2–300 K at an applied magnetic field of 0.1 T. The diamagnetic contributions of the samples were corrected using Pascal's constants.

**Synthesis of *N*-Methyliminobis(methylenephosphonic acid) (**H<sub>3</sub>L**).** The diphosphonic acid was prepared by a Mannich type reaction according to the procedures previously described.<sup>17</sup> Methylamine (Aldrich, 50 mmol) was mixed with hydrochloric acid (EM Science, 8.6 cm<sup>3</sup>), deionized water (5 mL), and phosphoric acid (Aldrich, 200 mmol). The mixture was allowed to reflux at 120 °C for 1 h, then paraformaldehyde (Aldrich, 150 mmol) was added in small portions over a period of 1 h, and the mixture was then refluxed for an additional 1 h. Removal of solvents afforded 6.5 g of a white powder of *N*-methyliminobis(methylenephosphonic acid) (yield 59.0%). Its purity was confirmed by NMR measurements and elemental analysis.  $^{31}\text{P}$  NMR shows only one single peak at 8.088 ppm.  $^1\text{H}$  NMR: 3.092 ppm ( $\text{CH}_3$ , 3H, s), 3.470 ppm ( $-\text{CH}_2-$ , d, 4H,  $J_{\text{H-P}} = 12.9$  Hz). Elemental analysis for  $\text{C}_3\text{H}_{11}\text{NO}_6\text{P}_2$ : C, 16.31; H, 5.22; N, 6.65; P, 28.08. Calcd: C, 16.45; H, 5.06; N, 6.40; P, 28.27.

**Preparation of  $\text{Mn}(\text{H}_3\text{L})_2\cdot 2\text{H}_2\text{O}$  (Complex **1**).** The manganese phosphonate was synthesized by a layering technique. Manganese acetate (Matheson Coleman & Bell Manufacturing Chemists) (0.5 mmol) dissolved in 5 mL of 1:1 (volume ratio) deionized water–ethyl alcohol mixed solvent was layered on top of the *N*-methyliminobis(methylenephosphonic acid) (1.0 mmol) dissolved in 5.0 mL of the same EtOH/H<sub>2</sub>O solvent. After 2 weeks, small light pink crystals grew on the wall of the glass tube and a voluminous white powder formed on the bottom of the glass tube, yield 65.7% (crystals and powder). The powder and single crystals have the same composition, as confirmed by elemental analysis, TGA, X-ray powder pattern, and magnetic measurements. Elemental analysis for complex **1**: C, 13.33; H, 4.45; N, 5.48; P, 23.74. Calcd: C, 13.67; H, 4.59; N, 5.32; P, 23.50.

**Synthesis of  $\text{Zn}_3(\text{HL})_2$  (Complex **2**).** The zinc complex was prepared by hydrothermal reactions. A mixture of 1.5 mmol of zinc acetate (Fisher Chem.), 1 mmol of *N*-methyliminobis(methylenephosphonic acid), and 10 mL of deionized water was heated at 165 °C for 4 days. Colorless crystals were recovered in ca. 35% yield. Elemental analysis for complex **2**: C, 11.30; H, 2.42; N, 4.55; P, 19.91. Calcd: C, 11.47; H, 2.57; N, 4.46; P, 19.72. Attempts

- (17) (a) Moedritzer, K.; Irani, R. R. *J. Org. Chem.* **1966**, *31*, 1603. (b) Soroka, M.; Mastalerz, P. *Pol. J. Chem.* **1976**, *50*, 661. (c) Oleksysyn, J.; Gruszecka, E.; Kafarski, P.; Mastalerz, P. *Monatsh. Chem.* **1982**, *113*, 1138.

**Table 1.** Crystal Data and Structure Refinements for Complexes **1** and **2**<sup>a</sup>

compound	<b>1</b>	<b>2</b>
empirical formula	C <sub>6</sub> H <sub>24</sub> MnN <sub>2</sub> O <sub>14</sub> P <sub>4</sub>	C <sub>6</sub> H <sub>16</sub> Zn <sub>3</sub> N <sub>2</sub> O <sub>12</sub> P <sub>4</sub>
fw	527.09	628.20
space group	<i>P</i> $\bar{1}$ (No. 2)	<i>P</i> 2 <sub>1</sub> / <i>n</i> (No. 14)
<i>a</i> /Å	9.224(3)	7.7788(9)
<i>b</i> /Å	9.780(3)	17.025(2)
<i>c</i> /Å	10.554(3)	13.041(2)
$\alpha$ /deg	82.009(6)	90.0
$\beta$ /deg	74.356(6)	94.597(2)
$\gamma$ /deg	89.853(6)	90.0
<i>V</i> , Å <sup>3</sup>	907.4(5)	1721.5(3)
<i>Z</i>	2	4
<i>D</i> <sub>calcd</sub> , g cm <sup>-3</sup>	1.929	2.424
$\mu$ , mm <sup>-1</sup>	1.155	4.584
GOF on <i>F</i> <sup>2</sup>	0.996	1.085
R1, wR2 [ <i>I</i> > 2 $\sigma$ ( <i>I</i> )]	0.0668, 0.1825	0.0434, 0.1047
R1, wR2 (all data)	0.0975, 0.2158	0.0552, 0.1124

$$^a R1 = \sum |F_o| - |F_c| / \sum |F_o|, wR2 = \{ \sum w[(F_o)^2 - (F_c)^2]^2 / \sum w(F_o)^2 \}^{1/2}.$$

to synthesize a manganese(II) compound by hydrothermal reactions at 165 °C produced only a clear solution, and no crystals or powder were isolated. This is probably due to the solubility of the manganese(II) phosphonate in pure water.

**Crystal Structure Determination.** Single crystals were mounted on a Bruker Smart CCD using Mo K $\alpha$  radiation ( $\lambda = 0.71069$  Å) and a graphite monochromator at 110(2) K. The cell constants were indexed from reflections obtained from 60 frames collected with 10 s exposure per frame. A hemisphere of data (1271 frames at 5 cm detector distances) was collected by the narrow-frame method with scan widths of 0.30° in  $\omega$  and exposure time of 30 s per frame. The first 50 frames were re-collected in the end of data collection to assess the stability of the crystal, and it was found that the decay in intensity was less than 1%. The data were corrected for Lorentz factor, polarization, air absorption, and absorption due to variations in the path length through the detector faceplate. An empirical absorption correction based on the  $\psi$  scan method was also applied.

The space group was uniquely determined to be *P* $\bar{1}$  (No. 2) for **1** and *P*2<sub>1</sub>/*n* (No. 14) for **2**. The structures were solved using direct methods (SHELXTL) and refined by least-squares methods with atomic coordinates and anisotropic thermal parameters for all non-hydrogen atoms.<sup>18</sup> All hydrogen atoms, except those for water molecules, were generated geometrically, assigned fixed isotropic thermal parameters, and included in the structure factor calculations. The hydrogen atoms for the water molecules in both complexes were located from difference Fourier maps and were refined isotropically. The final difference Fourier maps showed featureless residual peaks of 1.360 (for complex **1**, 0.95 Å from the O(7) atom) and 1.446 e $\cdot$ Å<sup>-3</sup> (for complex **2**, 0.03 Å from the Zn(2) atom), respectively. Some of the data collection and refinement parameters are summarized in Table 1. Important bond lengths and angles for the two complexes are listed in Table 2. More details on the crystallographic studies as well as atom displacement parameters are given in the Supporting Information.

## Results

**Crystal Structure of Mn(H<sub>3</sub>L)<sub>2</sub>·2H<sub>2</sub>O (**1**).** An ORTEP representation of the asymmetric unit of complex **1** is shown in Figure 1. Both Mn1 and Mn2 atoms lie on centers of symmetry and are octahedrally coordinated by four oxygen

**Table 2.** Selected Bond Lengths (Å) and Angles (deg) for Complexes **1** and **2**<sup>a</sup>

[Mn{CH <sub>3</sub> NH(CH <sub>2</sub> PO <sub>3</sub> H) <sub>2</sub> } <sub>2</sub> ·2H <sub>2</sub> O ( <b>1</b> )			
Mn(1)–O(5)#1	2.171(5)	Mn(1)–O(5)	2.171(5)
Mn(1)–O(7)#1	2.175(5)	Mn(1)–O(7)	2.175(5)
Mn(1)–O(1)#1	2.211(4)	Mn(1)–O(1)	2.211(4)
Mn(2)–O(8)	2.150(4)	Mn(2)–O(8)#2	2.150(4)
Mn(2)–O(10)#2	2.196(5)	Mn(2)–O(10)	2.196(5)
Mn(2)–O(4)#3	2.206(4)	Mn(2)–O(4)#4	2.206(4)
P(1)–O(1)	1.495(5)	P(1)–O(2)	1.537(5)
P(1)–O(3)	1.558(5)	P(1)–C(1)	1.818(7)
P(2)–O(4)	1.501(5)	P(2)–O(5)	1.502(5)
P(2)–O(6)	1.587(5)	P(2)–C(2)	1.825(7)
P(3)–O(7)	1.513(5)	P(3)–O(8)	1.518(4)
P(3)–O(9)	1.573(5)	P(3)–C(5)	1.835(7)
P(4)–O(10)	1.511(5)	P(4)–O(12)	1.534(5)
P(4)–O(11)	1.544(5)	P(4)–C(4)	1.828(7)
Hydrogen Bonding:			
O(1W)···O(1W)#6	2.751	O(1W)···O(9)	2.729
O(2W)···O(2)	2.603	O(2W)···O(2W)#7	2.721
O(2W)···O(6)#1	2.911	O(2)···O(9)#1	2.737
O(3)···O(12)#8	2.571	O(6)···O(12)#4	2.607
N(1)···O(8)#4	2.975	N(1)···O(10)#5	2.856
N(2)···O(1)	2.841	N(2)···O(5)#1	2.987
O(5)#1–Mn(1)–O(5)	180.000(1)	O(5)#1–Mn(1)–O(7)#1	92.40(17)
O(5)–Mn(1)–O(7)#1	87.60(17)	O(5)#1–Mn(1)–O(7)	87.60(17)
O(5)–Mn(1)–O(7)	92.40(17)	O(7)#1–Mn(1)–O(7)	180.0(2)
O(5)#1–Mn(1)–O(1)#1	94.03(17)	O(5)–Mn(1)–O(1)#1	85.97(17)
O(7)#1–Mn(1)–O(1)#1	83.44(17)	O(7)–Mn(1)–O(1)#1	96.56(17)
O(5)#1–Mn(1)–O(1)	85.97(16)	O(5)–Mn(1)–O(1)	94.03(17)
O(7)#1–Mn(1)–O(1)	96.56(17)	O(7)–Mn(1)–O(1)	83.44(17)
O(1)#1–Mn(1)–O(1)	180.000(1)	O(8)–Mn(2)–O(8)#2	180.000(1)
O(8)–Mn(2)–O(10)#2	88.05(17)	O(8)#2–Mn(2)–O(10)#2	91.95(17)
O(8)–Mn(2)–O(10)	91.95(17)	O(8)#2–Mn(2)–O(10)	88.05(17)
O(10)#2–Mn(2)–O(10)	180.00(3)	O(8)–Mn(2)–O(4)#3	91.10(17)
O(8)#2–Mn(2)–O(4)#3	88.90(17)	O(10)#2–Mn(2)–O(4)#3	95.16(16)
O(10)–Mn(2)–O(4)#3	84.84(16)	O(8)–Mn(2)–O(4)#4	88.90(17)
O(8)#2–Mn(2)–O(4)#4	91.10(17)	O(10)#2–Mn(2)–O(4)#4	84.84(16)
O(10)–Mn(2)–O(4)#4	95.16(16)	O(4)#3–Mn(2)–O(4)#4	180.0(2)
P(1)–O(1)–Mn(1)	133.6(3)	P(2)–O(4)–Mn(2)#5	139.3(3)
P(2)–O(5)–Mn(1)	136.5(3)	P(3)–O(7)–Mn(1)	141.1(3)
P(3)–O(8)–Mn(2)	134.2(3)	P(4)–O(10)–Mn(2)	137.7(3)
Zn <sub>3</sub> {CH <sub>3</sub> NH(CH <sub>2</sub> PO <sub>3</sub> H) <sub>2</sub> } <sub>2</sub> ( <b>2</b> )			
Zn(1)–O(12)#1	1.931(3)	Zn(1)–O(7)#2	1.936(3)
Zn(1)–O(5)#3	1.947(3)	Zn(1)–O(3)	1.975(3)
Zn(2)–O(9)#4	1.927(3)	Zn(2)–O(11)#3	1.929(3)
Zn(2)–O(6)#5	1.929(3)	Zn(2)–O(2)	1.966(3)
Zn(3)–O(8)#2	1.894(3)	Zn(3)–O(1)#6	1.944(3)
Zn(3)–O(10)	1.962(3)	Zn(3)–O(4)	1.965(3)
P(1)–O(1)	1.512(3)	P(1)–O(2)	1.526(3)
P(1)–O(3)	1.541(3)	P(1)–C(1)	1.828(4)
P(2)–O(5)	1.521(3)	P(2)–O(4)	1.524(3)
P(2)–O(6)	1.529(3)	P(2)–C(2)	1.826(4)
P(3)–O(9)	1.511(3)	P(3)–O(8)	1.520(3)
P(3)–O(7)	1.525(3)	P(3)–C(4)	1.845(4)
P(4)–O(11)	1.514(3)	P(4)–O(12)	1.515(3)
P(4)–O(10)	1.541(3)	P(4)–C(5)	1.830(4)
N(1)···O(10)	2.784	N(2)···O(3)	2.845
N(1)–H(11A)···O(10)	171.0	N(2)–H(12A)···O(3)	169.1
O(12)#1–Zn(1)–O(7)#2	101.77(13)	O(12)#1–Zn(1)–O(5)#3	114.58(13)
O(7)#2–Zn(1)–O(5)#3	101.63(12)	O(12)#1–Zn(1)–O(3)	112.23(12)
O(7)#2–Zn(1)–O(3)	117.02(12)	O(5)#3–Zn(1)–O(3)	109.24(12)
O(9)#4–Zn(2)–O(11)#3	104.06(13)	O(9)#4–Zn(2)–O(6)#5	107.27(12)
O(11)#3–Zn(2)–O(6)#5	114.25(13)	O(9)#4–Zn(2)–O(2)	110.05(12)
O(11)#3–Zn(2)–O(2)	110.64(12)	O(6)#5–Zn(2)–O(2)	110.30(12)
O(8)#2–Zn(3)–O(1)#6	103.34(13)	O(8)#2–Zn(3)–O(10)	117.07(13)
O(1)#6–Zn(3)–O(10)	118.76(12)	O(8)#2–Zn(3)–O(4)	108.97(13)
O(1)#6–Zn(3)–O(4)	107.04(13)	O(10)–Zn(3)–O(4)	101.10(12)

<sup>a</sup> Symmetry transformations used to generate equivalent atoms: For complex **1**: #1  $-x + 1, -y + 1, -z + 1$ ; #2  $-x + 2, -y, -z + 1$ ; #3  $x, y - 1, z$ ; #4  $-x + 2, -y + 1, -z + 1$ ; #5  $x, y + 1, z$ ; #6  $-x + 1, -y, z - z$ ; #7  $-x + 1, -y + 1, z$ ; #8  $-x + 2, -y + 1, -z$ . For complex **2**: #1  $x - 1/2, -y + 3/2, z + 1/2$ ; #2  $x - 1, y, z$ ; #3  $x + 1/2, -y + 3/2, z + 1/2$ ; #4  $-x + 3/2, y - 1/2, -z + 1/2$ ; #5  $x + 1, y, z$ ; #6  $x - 1/2, -y + 3/2, z - 1/2$ ; #7  $-x + 3/2, y + 1/2, -z + 1/2$ ; #8  $x + 1/2, -y + 3/2, z - 1/2$ .

(18) Sheldrick, G. M. *SHELXTL*, version 5.03; Siemens Analytical X-ray Instruments: Madison, WI, 1995. Sheldrick, G. M. *SHELX-96 Program for Crystal Structure Determination*; Bruker-AXS: Madison, WI, 1996.

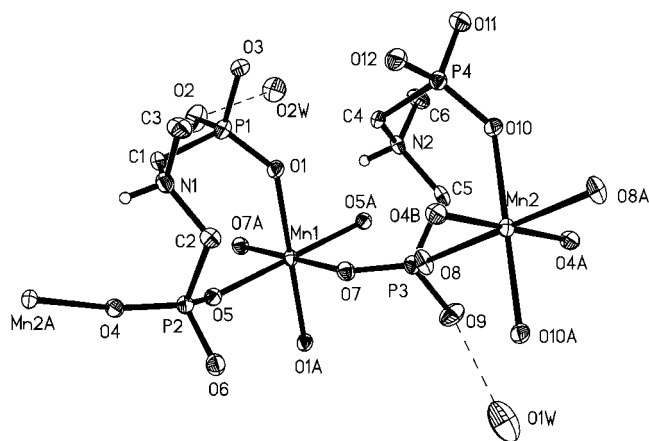


**Figure 1.** ORTEP representation of the asymmetry unit of complex **1**. Thermal ellipsoids are drawn at 50% probability. The dotted lines indicate hydrogen bonds.

atoms from two chelating ligands and two phosphonate oxygen atoms from two neighboring  $\text{Mn}(\text{H}_3\text{L})_2$  units. Each ligand acts as a tridentate ligand by chelating with one manganese atom and bridging with another  $\text{Mn}(\text{II})$  ion, thus forming two different kinds of eight-membered chelate rings. One such ring is composed of Mn1, O1, P1, C1, N1, C2, P2, O5 atoms; the other one contains Mn2, O8, P3, C5, N2, C4, P4, O10 atoms (Figure 1). The Mn–O distances range from 2.150(4) to 2.211(4) Å. The nitrogen atom and both phosphonate groups of the ligand are 1H-protonated, thus each ligand carries a negative charge of one, and two ligands are needed to balance the two positive charges of a  $\text{Mn}(\text{II})$  ion. The lattice water molecules (O1W, O2W) are not coordinated to the  $\text{Mn}(\text{II})$  ions, but form strong hydrogen bonds with phosphonate oxygen atoms (O1W $\cdots$ O9 2.729 Å, O2W $\cdots$ O2 2.603 Å, and O2W $\cdots$ O6 2.911 Å) or with neighboring water molecules (O1W $\cdots$ O1W 2.751 Å and O2W $\cdots$ O2W 2.721 Å) (Table 2).

The  $\text{Mn}(\text{H}_3\text{L})_2$  units are interconnected by bridging phosphonate groups, forming a 2D metal phosphonate layer along the (002) plane (Figure 2a). The bridging phosphonate groups (P2, O4, O5 and P3, O7, O8) form 16-membered rings with manganese atoms (2Mn1, 2Mn2, 2P2, 2O4, 2O5, 2P3, 2O7, 2O8) (Figure 2b). The unidentate-coordinating phosphonate groups (P1 and P4) are attached above and below the plane. The methyl groups are oriented toward the cavity created by the 16-membered rings as shown in Figure 2a. Hydrogen bonds are formed between phosphonate oxygen atoms within a layer (O2 $\cdots$ O9 2.737 Å and O6 $\cdots$ O12 2.607 Å), as well as between nitrogen atoms and phosphonate oxygen atoms within the layer (N1–H11a $\cdots$ O8 2.975 Å (146.8°), N1–H11a–O(10) 2.856 Å (126.6°); N2–H22a $\cdots$ O1 2.841 Å (149.1°), N2–H22a $\cdots$ O5 2.987 Å (125.4°)) (Table 2).

These metal phosphonate layers are further interlinked by interlayer hydrogen bonds (Figure 3). In addition to the hydrogen bonds between phosphonate oxygen atoms and lattice water molecules discussed above, there are also strong hydrogen bonds formed between phosphonate oxygen atoms from two neighboring layers (O3 $\cdots$ O12 2.571(9) Å) (Table 2). The O3–H3D $\cdots$ O12 bond angle is 177.20(3)°. Strong hydrogen bond formation has been found to exist in the

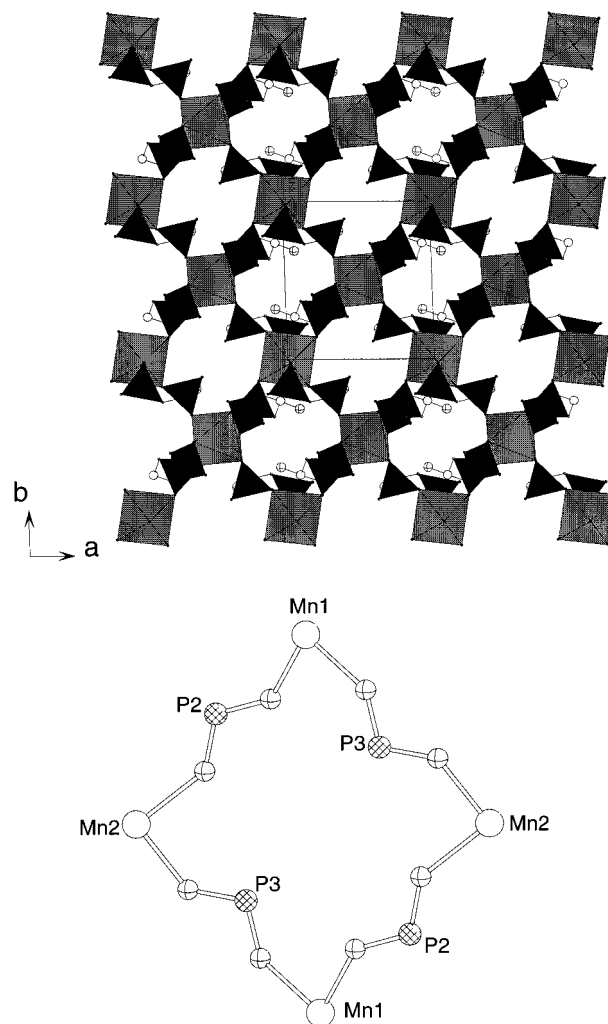


**Figure 2.** (a) Polyhedral representation of a manganese(II) phosphonate layer along the [002] plane.  $\text{MnO}_6$  octahedra and C– $\text{PO}_3$  tetrahedra are shaded in gray and black, respectively. N and methyl C atoms are shown as open and crossed circles, respectively. (b) One 16-membered ring of  $(-\text{Mn}-\text{O}-\text{P}-\text{O})_4$ . Mn, P and O atoms are represented by large (open), medium (hatched), and small (crossed) circles, respectively.

parent ligand *N*-methyliminobis(methylenephosphonic acid) and its derivatives,<sup>16,19</sup> as well as phosphonic acids attached to aza-crown ethers, resulting in the formation of “macrocylic leaflets”.<sup>4,20</sup>

**Crystal Structure of  $\text{Zn}_3(\text{HL})_2$  (2).** The structure of the zinc complex is different from the manganese complex in that it features a porous 3D network structure. As shown in Figure 4, the asymmetric structural unit of the zinc complex contains three zinc atoms and two ligands. Each zinc atom is tetrahedrally coordinated by four phosphonate oxygen atoms from four ligands. The Zn–O distances range from 1.894(3) to 1.975(3) Å (Table 2), which are comparable with those of zinc diphosphonates reported before.<sup>9</sup> Unlike in the Mn complex, each ligand in the zinc complex acts as a hexadentate ligand and bridges with six zinc atoms. Both phosphonate groups of the ligand are completely deprotonated.

(19) (a) Daly, J. J.; Wheatley, J. J. *J. Chem. Soc. A* **1967**, 212. Makaranets, B. I.; Polynova, T. N.; Bel'skii, V. K.; Il'ichev, S. A.; Porai-Koshits, M. A. *J. Struct. Chem.* **1985**, 26, 761.

(20) Sharma, C. V. K.; Mao, J.-G.; Clearfield A. *Chem. Mater.*, submitted.

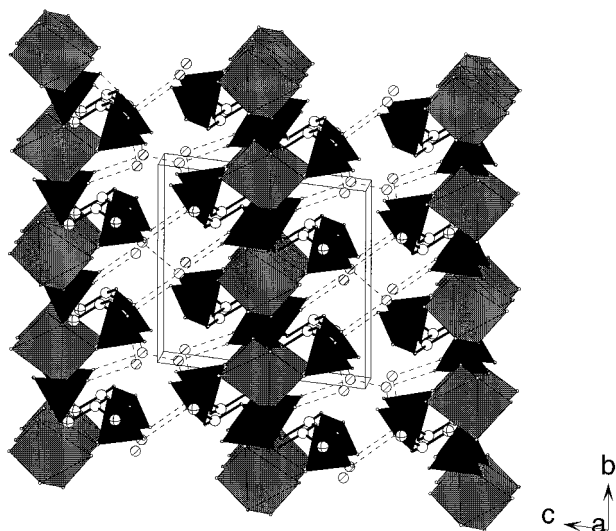


**Figure 3.** View of crystal structure of complex **1** along the *a* axis.  $\text{MnO}_6$  octahedra and  $\text{C}-\text{PO}_3$  tetrahedra are shaded in gray and black, respectively. N, methyl C, and lattice water atoms are shown as open, crossed, and hatched circles, respectively. The dotted lines indicate hydrogen bonds.

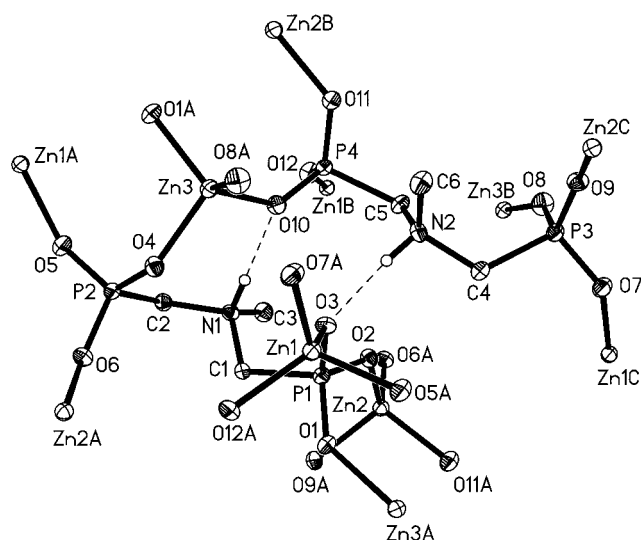


**Figure 4.** ORTEP representation of the asymmetry unit of complex **2**. Thermal ellipsoids are drawn at 50% probability. The dotted lines represent hydrogen bonds.

nated. The amine group, however, is still protonated; thus each ligand carries three negative charges, requiring a metal-to-ligand ratio of 3:2. The protonated nitrogen atoms form hydrogen bonds with phosphonate oxygen atoms ( $\text{N1}-\text{H11A}\cdots\text{O10}$  2.784 Å (171.0°);  $\text{N2}-\text{H12A}\cdots\text{O3}$  2.845 Å (169.1°)) (Figure 4).

The  $\text{ZnO}_4$  tetrahedra are interconnected by phosphonate groups, resulting in the formation of a complex 3D network with various voids as shown in Figure 5. These voids are created by 8-, 12-, and 16-membered rings (Figure 6). Each eight-membered ring contains two zinc atoms and two phosphonate groups,  $\{-\text{Zn}-\text{O}-\text{P}-\text{O}-\}_2$ ; such a ring adopts a pseudo-chair conformation.<sup>13</sup> A 12-membered ring is formed by three zinc atoms and three phosphonate groups, whereas a 16-membered ring is composed of four zinc atoms and four phosphonate groups.

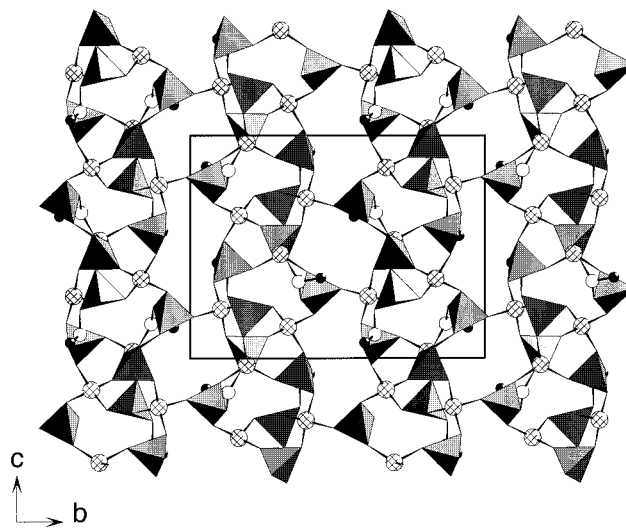


**Figure 5.** View of crystal structure of complex **2** along the *a* axis. The phosphonate groups are represented by tetrahedra. Zn, N, and methyl C atoms are shown as large (hatching), medium (open) and small black circles, respectively.

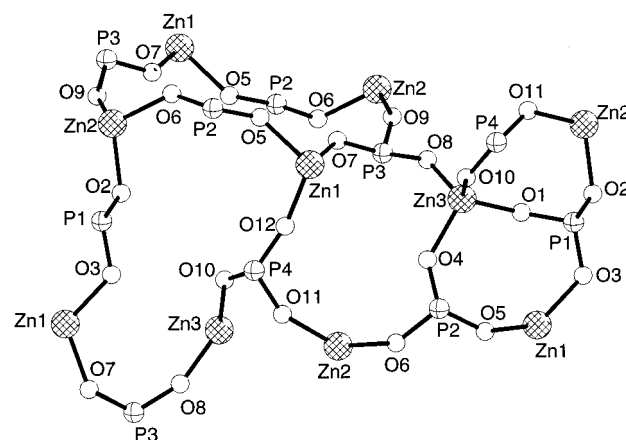


**Figure 6.** 8-, 12- and 16-membered rings in complex **2**. Zn, P, O atoms are represented by large (hatched), medium (crossed), and small (open) circles, respectively.

**Thermogravimetric Study.** A TGA diagram of complex **1** shows four major weight losses. The first step is the loss of two lattice water molecules, completed at 204 °C. The weight loss of 7.00% is in good agreement with the calculated value (6.80%). There are two processes taking place between 300 and 600 °C: first, the release of two water molecules formed by the condensation of hydrogen phosphonate groups; second, the pyrolysis of the organic group. However, these two processes overlap. The weight loss continues after 600 °C, even to 1000 °C. The final product is mainly  $\text{Mn}(\text{PO}_3)_2$ , a metal metaphosphate, and the calculated weight loss of 59.61% is larger than the observed one (45.52%); thus the reaction is not complete at 1000 °C. The TGA diagram for complex **2** is much simpler. There are two steps of weight loss that are overlapped; first, the burning of organic groups between 450 and 580 °C; second, from 580 to 823.0 °C. The total weight loss is 15.5%, which is in good agreement with the calculated weight loss of 15.92% if the final products are assumed to be zinc metaphosphate ( $\text{Zn}(\text{PO}_3)_2$ ) and zinc oxide in a 2:1 ratio.

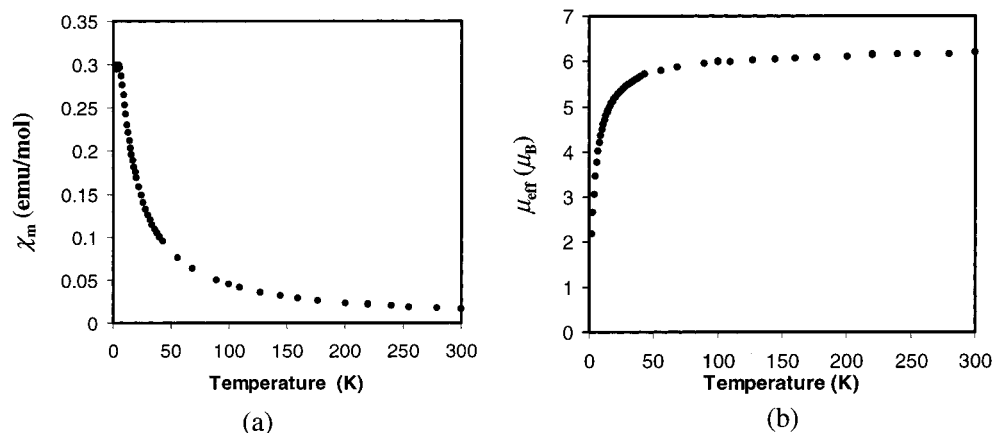
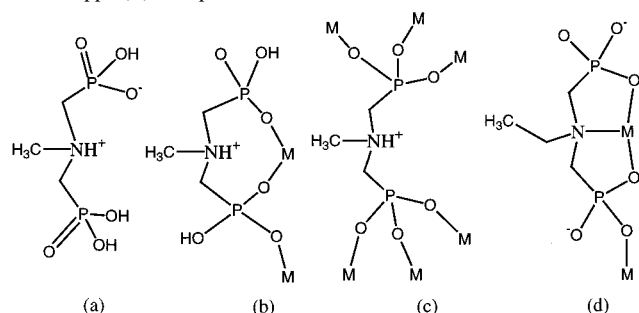


**Figure 7.** Magnetic property measurements for complex **1**: (a) plot of the molar susceptibility ( $\chi_m$ ) as a function of temperature ( $T$ ); (b) plot of the effective magnetic moment ( $\mu_{\text{eff}}$ ) as a function of temperature ( $T$ ).

**Scheme 1.** Ligand  $H_4L$  and Its Coordination Modes in Complexes **1** and **2**, as Well as That of *N*-Ethyliminobis(methylenephosphonic acid) in Its Copper(II) Complex



**Magnetic Property.** The results for complex **1** are shown in Figure 7. The molar susceptibility of the manganese(II) complex increases with the decrease in temperature (Figure 7a). The dependence of the effective magnetic moment ( $\mu_{\text{eff}}$ ) for complex **1** with the temperature is shown in Figure 7b. At room temperature the measured  $\mu_{\text{eff}}$  of  $6.12 \mu_B$  corresponds to a high-spin manganese(II) ion ( $5.92 \mu_B$ ). At 2 K, the  $\mu_{\text{eff}}$  value is decreased to  $2.19 \mu_B$ . The measured Curie constant is  $4.935 \text{ emu-K/mol}$ , which is slightly larger than the calculated value ( $4.38 \text{ emu-K/mol}$ ). The  $\theta$  value is calculated to be  $-9.925 \text{ K}$ ; thus there is significant anti-ferromagnetic interaction between manganese(II) ions bridged by phosphonate groups ( $Mn \cdots Mn$   $6.713(1) \text{ \AA}$ ). The interlayer distance is calculated to be  $10.054 \text{ \AA}$ , and we assumed that the interlayer magnetic interaction is negligible.

## Discussion

Reaction of *N*-methyliminobis(methylenephosphonic acid) ( $H_4L$ ) with manganese(II) acetate via a layering technique yielded a layered metal phosphonate,  $Mn(H_3L)_2 \cdot 2H_2O$ , **1**, which has a M/L ratio of 1:2. Hydrothermal reaction of this ligand with zinc(II) acetate afforded a 3:2 (M/L) complex with a 3D network structure,  $Zn_3(HL)_2$ , **2**. Scheme 1 shows the ligand  $H_4L$  (a) and different coordination modes it adopts in its manganese(II) (b) and zinc(II) (c) complexes, as well as the coordination mode of *N*-ethyliminobis(methylenephosphonic acid) in its copper(II) complex (d). *N*-methyliminobis(methylenephosphonic acid) occurs in a zwitterionic

form (Scheme 1a), which is a common form for phosphonic acids containing amine groups.<sup>4,9,16,20</sup> These zwitterions are interconnected into a 3D network based on tetramers through strong intermolecular hydrogen bonding [ $2.446(2)$ ,  $2.525(2)$ , and  $2.572(2) \text{ \AA}$ ].<sup>16</sup> Upon reaction with manganese(II) acetate under weak acidic conditions at room temperature, one more proton on another phosphonate group is deprotonated; thus a complex with 1:2 (M/L) is formed. The ligand adopts a tridentate chelate and bridging coordinate mode (Scheme 1b) to form a layer structure. The uncoordinated phosphonate oxygens are available for intra- and interlayer hydrogen bonding. Under hydrothermal conditions at a higher temperature ( $165 \text{ }^\circ\text{C}$ ), all of the protons on both phosphonate groups have been removed, but the amine group is still protonated. The three negatively charged ligand forms a 3:2 (M/L) complex with zinc(II) acetate,  $Zn_3(HL)_2$ , **2**. HL in the zinc complex acts as a hexadentate ligand, bridging with six zinc ions (Scheme 1c). The structure of the zinc complex is very different from the layer structure proposed by the solution studies.<sup>16</sup> Under weak basic conditions (pH  $\sim 8$ ), the proton on the amine group can be deprotonated and a tridentate chelating mode (Scheme 1d) can be adopted, as reported in the copper complex with ethylaminebis(methylphosphonate).<sup>15</sup> The remaining phosphonate oxygen atoms in this compound are connected to Cs(I) ions as  $Cs_2CO_3$  was used to increase the pH. Deprotonation of the amine groups is also dependent on the affinity of the metal ions for the nitrogen atom and the properties of the chelate rings. In metal polyaminephosphonates, such as those in which the phosphonate groups are attached to ethylenediamine or polyaza-crown ether, the nitrogen atoms of the ligand are coordinated to the metal ion even under weak acidic conditions.<sup>12,21</sup>

In the recent past we have prepared a number of complexes of mono-, di-, and triphosphonic acids, with nitrilotris(methylphosphonic acid) ( $3H_6N$ ) representing the triphosphonic acid. It is clear that the degree of deprotonation and the resultant hydrogen bonding determines the type of complex formed. The phosphorylated crown ethers, *N*-(phos-

(21) Kotek, J.; Hermann, P.; Císarová, I.; Rohovec, J.; Lukeš, I. *Inorg. Chim. Acta* **2001**, *317*, 324.

phonomethyl)-aza-18-crown-6 and *N*-(phosphonomethyl)-aza-15-crown-5 form one-dimensional polymeric arrays through hydrogen-bonded and coordination-bonded self-assembly.<sup>4b,22</sup> 3H<sub>6</sub>N forms unique three-dimensional hexagonal structures when a single proton is transferred to an amine. This reaction triggers formation of a hexagonal 3D hydrogen bonded array that encapsulates the amines as templates.<sup>23</sup> If two protons are removed, one-dimensional chain structures are obtained.<sup>23</sup> By choice of the proper template, layered compounds may also be prepared.<sup>23</sup> The exploration of divalent metal complexes with these ligands has produced several new structure types as described here and in several recent manuscripts.<sup>7,20,24</sup> Further systematic

---

(22) Clearfield, A.; Sharma, C. V. K.; Zhang, B. *Chem. Mater.* **2001**, *13*, 3099.

(23) (a) Sharma, C. V. K.; Hessheimer, A. J.; Clearfield, A. *Polyhedron* **2001**, *20*, 2095. (b) Sharma, C. V. K.; Clearfield, A. *J. Am. Chem. Soc.* **2000**, *122*, 4394.

removal of the protons sequentially from these and other phosphonic acid ligands is in progress to uncover other possible structure types.

**Acknowledgment.** We acknowledge with thanks the financial support from the Robert A. Welch Foundation through Grant No. A673 and the Department of Energy, Basic Sciences Division, through Grant No. DOE 448071-00001. We thank Dr. Han-Hua Zhao for his help with the magnetic measurements.

**Supporting Information Available:** X-ray crystallographic files in CIF format for the structure determination of Mn(H<sub>3</sub>L)<sub>2</sub>·2H<sub>2</sub>O (**1**) and Zn<sub>3</sub>(HL)<sub>2</sub> (**2**). This material is available free of charge via the Internet at <http://pubs.acs.org>.

IC011202E

---

(24) Sharma, C. V. K.; Clearfield, A.; Cabeza, A.; Aranda, M. A. G.; Bruque, S. *J. Am. Chem. Soc.* **2001**, *123*, 2885.